Fluidity of Bound Hydration Layers
Uri Raviv, *et al.*
Science **297**, 1540 (2002);
DOI: 10.1126/science.1074481

Science (print ISSN 0036-8075; online ISSN 1095-9203) is published weekly, except the last week in December, by the American Association for the Advancement of Science, 1200 New York Avenue NW, Washington, DC 20005.

11. Materials and methods are available as supporting material on *Science* Online.
12. L. M. Demers *et al*., *Anal. Chem.* **72**, 5535 (2000).
13. R. L. McCreery, *Raman Spectroscopy for Chemical Analysis* (Wiley, New York, 2000).
14. G. C. Schatz, R. P. Van Duyne, in *Handbook of Vibrational Spectroscopy*, J. M. Chalmers, P. R. Griffiths, Eds. (Wiley, New York, 2002), pp. 759–774.
15. A. Campion, P. Kambhampati, *Chem. Soc. Rev.* **27**, 241 (1998).
16. S. R. Emory, S. Nie, *J. Phys. Chem. B* **102**, 493 (1998).
17. M. D. Musick, C. D. Keating, M. H. Keefe, M. J. Natan, *Chem. Mater.* **9**, 1499 (1997).
18. A. M. Michaels, M. Nirmal, L. E. Brus, *J. Am. Chem. Soc.* **121**, 9932 (1999).
19. S. J. Park, T. A. Taton, C. A. Mirkin, *Science* **295**, 1503 (2002).
20. M. Bruchez Jr., M. Moronne, P. Gin, S. Weiss, A. P. Alivisatos, *Science* **281**, 2013 (1998).
21. W. C. W. Chan, S. Nie, *Science* **281**, 2016 (1998).
22. L. He *et al*., *J. Am. Chem. Soc.* **122**, 9071 (2000).
23. I. Willner, F. Patolsky, J. Wasserman, *Angew. Chem. Int. Ed.* **40**, 2261 (2001).
24. H. Mattoussi *et al*., *J. Am. Chem. Soc.* **122**, 12142 (2000).
25. S. Pathak, S. K. Choi, N. Arnheim, M. E. Thompson, *J. Am. Chem. Soc.* **123**, 4103 (2001).
26. Y. Cui, Q. Wei, H. Park, C. M. Lieber, *Science* **293**, 1289 (2001).
27. C. M. Niemeyer, *Angew. Chem. Int. Ed.* **40**, 4128 (2001).

28. We acknowledge R. L. Letsinger and L. G. Zhang for helpful discussions. C.A.M. acknowledges the Air Force Office of Scientific Research (AFOSR), the Defense Advanced Research Projects Agency (DARPA), and the NSF for support of this research. R.J. is grateful for the support of the American Chemical Society Cognis Fellowship in Colloid and Surface Chemistry.

Supporting Online Material
www.sciencemag.org/cgi/content/full/297/5586/1536/DC1
Materials and Methods
Schemes S1 and S2
Figs. S1 to S3

12 June 2002; accepted 31 July 2002

Fluidity of Bound Hydration Layers

Uri Raviv[1] and Jacob Klein[1,2]*

We have measured the shear forces between solid surfaces sliding past each other across aqueous salt solutions, at pressures and concentrations typical of naturally occurring systems. In such systems the surface-attached hydration layers keep the compressed surfaces apart as a result of strongly repulsive hydration forces. We find, however, that the bound water molecules retain a shear fluidity characteristic of the bulk liquid, even when compressed down to films 1.0 ± 0.3 nanometer thick. We attribute this to the ready exchange (as opposed to loss) of water molecules within the hydration layers as they rub past each other under strong compression.

The presence of water molecules tightly bound to ions or ionized surfaces in aqueous electrolytes leads to strong repulsion when they approach each other to within a few nanometers or less (*1*–*4*). This effect is thought to arise from the reluctance of the ions or surfaces to shed their hydration sheath (*3*–*6*). It can dominate the double-layer repulsion/van der Waals attraction mechanisms [accounted for in the classic DLVO (Derjaguin, Landau, Verwey, and Overbeek) theory (*7*)] and is particularly important at the high salt concentrations (~0.1 M salt) found in nature. The way in which the properties of such hydration layers differ from those of bulk water has for decades excited much debate (*8*–*11*). At issue here is a simple question: Is the hydration layer surrounding such highly confined bound ions fluid, or is it highly viscous? The difference is crucial and is directly implicated in areas ranging from clay plasticity (*12*) and biolubrication (*13*) to gating of charge migration in DNA (*14*). In addition, many biological processes require shear and displacement of the final subnanometer layers of bound hydration layers before molecular contact or passage. These include interactions between ligands and receptors, transport within the very crowded intracellular environment (*15*) or through ion channels (*16*), and protein folding (*17*).

Extensive direct measurements, as well as modeling (*1*–*4*, *6*), have shed much light on equilibrium interactions of such bound hydration layers. In contrast, few direct measurements have been reported concerning their fluidity (*18*–*22*), particularly in the regime of the hydration sheaths, i.e., films of thickness $D = 7$ to 10 Å (*23*–*25*). We used a surface force balance (SFB) with extreme sensitivity in measuring shear interactions to probe directly the fluidity of aqueous electrolytes compressed and sheared between molecularly smooth mica surfaces. While our results confirm the long-established equilibrium hydration repulsion, they reveal at the same time that the bound water in the hydration layers remains extremely fluid under shear. This fluidity persists down to films in the range $D = D_c = 1.0 \pm 0.3$ nm, a thickness comparable to the size of hydrated ions in solution. Within such films, most of the confined water molecules are expected to be in bound hydration layers.

The SFB used has been described in detail (*26*). Its main features are schematically outlined in Fig. 1. We focus here on investigations of NaCl solutions, although preliminary studies on KNO_3 solutions (in the hydration repulsion regime) reveal very similar findings. The following results are based on several different experiments (different pairs of mica sheets), as well as on different contact positions within an experiment. Initial measurements in salt-free water were found to be crucial to establish the integrity and purity of the system. They were made to ensure the removal of any contaminant layers that adsorb on the mica while exposed to air (*2*, *27*, *28*), so as to attain true (mica-lattice/mica-lattice) contact between the surfaces (*29*). When the above behavior (*29*) could not be reproduced, as in our own earlier studies (*30*), subsequent measurements at high salt concentrations revealed high effective viscosities already at values of D as low as <2 to 3 nm, and these were attributed to contamination. A previous observation (*31*, *32*) of comparably high viscosities in salt solutions (~0.03 M) confined to $D < 2$ to 2.5 nm may have been related to this. Improvements in water purification and handling in the present study resolved this problem, as shown in figure 1 of (*33*) and in Fig. 1 of this study.

High-purity NaCl was then added to a concentration of 10^{-3} M (±10%), and normal and shear forces were measured as a further control. Mica loses K^+ ions to solution, leaving a net negative surface charge, and the resultant distribution of ions in the intersurface gap leads to a long-ranged osmotic repulsion followed by a jump-in to adhesive mica/mica contact, in close agreement with earlier studies (*3*, *4*) and in accord with DLVO theory (*7*) (Fig. 1). Such total extrusion of the low-salt electrolyte from between the adhering surfaces resembles that observed in salt-free water (*33*) and is thought to arise when the predominant hydroxonium H_3O^+ ions condense into the charged mica, retaining no hydrated layers at the surface (*3*, *4*).

Shear forces were measured as described recently (*33*). With the surfaces compressed down to separations of a few nm, the upper mica surface is made to move laterally back and forth, exactly parallel to the lower one at velocity v_s (Fig. 1 inset, upper trace). The shear forces F_s transmitted across the intersurface gap are simultaneously recorded as the surfaces further approach under slow thermal drift. No shear forces greater than the noise-limited sensitivity δF_s (±30 nN) are detected between the surfaces down to adhe-

[1]Weizmann Institute of Science, Rehovot 76100, Israel. [2]Physical and Theoretical Chemistry Laboratory, Oxford University, Oxford OX1 3QZ, UK.

*To whom correspondence should be addressed.

sive contact at $D = D_0 = 0.0 \pm 0.4$ nm. Analysis similar to that of (*33*) reveals that, as for the case of salt-free water (*33*), the effective viscosity of the 10^{-3} M salt solution remains close to its bulk value down to subnanometer-thick films and during the jump into contact at D_0. In all cases, the behavior described was fully reproducible on subsequent separations and approaches and consistent with earlier reports (*19*, *20*, *22*) on the viscosity of aqueous salt solutions confined to thicker films ($D \geq 1.8$ nm).

Following this, the surfaces were taken apart and the NaCl concentration increased to $(0.7 \pm 0.2) \times 10^{-2}$ M and subsequently to $(0.8 \pm 0.1) \times 10^{-1}$ M. At these salt concentrations hydration layers are bound at the surfaces, ensuring that on normal approach repulsive hydration forces overcome the van der Waals attraction at all surface separations (*3*, *4*). At both these concentrations we observed very similar shear force behavior. Figure 2 summarizes the normal force profiles and the shear measurements for both NaCl concentrations [$(0.7 \pm 2) \times 10^{-2}$ and $(0.8 \pm 0.1) \times 10^{-1}$ M]. The normal $F_n(D)$ profiles (Fig. 2A) confirm the results of earlier studies (*3*, *20*) showing the strong repulsion due to the confined surface-attached hydration layers at separations $D < \sim 2$ nm. Figure 2B [upper trace (a)] shows the back-and-forth motion of the upper mica surface. The lower traces (typical of many experiments) show shear force responses both at very large surface separations [trace (b), $D = \sim 9.6$ μm] as a control, and when strongly compressed down to $D = D_c$ in the range 1.0 ± 0.3 nm [traces (c) to (e)]. Within the scatter, traces (b) to (e) are very similar. The frequency (ν) dependence $F_s(\nu)$ of the shear force responses is shown in Fig. 2B on the right, with the arrows indicating the drive frequency of the upper mica surface. At this drive frequency the magnitude of F_s at D_c is within the noise level δF_s (± 30 nN) of its magnitude at macroscopic separations. In other words, the resistance to sliding even at these strongest compressions across the thinnest films is extremely weak, and within our sensitivity is indistinguishable from its value when the surfaces are far apart. This behavior was reversible and reproducible. The surfaces could be separated from $D = D_c$ to large separations, then recompressed to show again the absence of any detectable frictional force (*34*, *35*).

To examine the generality of our findings, we varied several parameters. Various (high) salt concentrations and different monovalent salts (NaCl and KNO_3) were used. The similarity of the results shows that for these two pairs, neither the different binding (monovalent) metal counterion nor the different co-ion affected the results. Shear rates were varied over the range 6 to 1200 s^{-1}. The mica sheets were mounted in different relative orientations, and the close similarity of results in all instances thus shows that this does not—within the scatter—affect the fluidity of the bound hydration layers. In two of the experiments mica pairs from the identical cleaved facet were used, and the results in those instances did not differ (within the scatter) either among themselves or from those where a pair of surfaces from a completely different mica sheet were used, suggesting a lack of sensitivity to the precise mica surface composition. Within the resolution and range of our experimental conditions, the fluidity of the bound hydration layers appears to be a general feature. In addition, stopping the sliding motion (at $D = D_c$) for periods up to 5 min and then restarting did not change the behavior. This indicates that any rearrangement of the layers over these time scales did not lead to significant differences.

We estimate an upper limit on the effective viscosity (η_{eff}) of the bound hydration layers (*36*) to be ≤ 0.08 Pa·s. Although this value is higher than the viscosity of the bulk electrolyte ($\sim 10^{-3}$ Pa·s), we stress that it is resolution-limited by $F_s \leq \delta F_s$ (~ 30 nN) and is therefore an upper limit, so that the actual value may be much closer to the bulk viscosity. The mean pressure in the flattened contact region of area A is $F_n/A = \sim 4$ atm at the typical normalized loads $F_n/R = 10^4$ μN/m associated with the high-compression regime (*36*).

These findings have interesting implications. The surface potential associated with the mica surfaces, deduced from the $F_n(D)$ profile, corresponds to a net surface charge of $\sim 1e/10$ nm^2. Although the precise state of

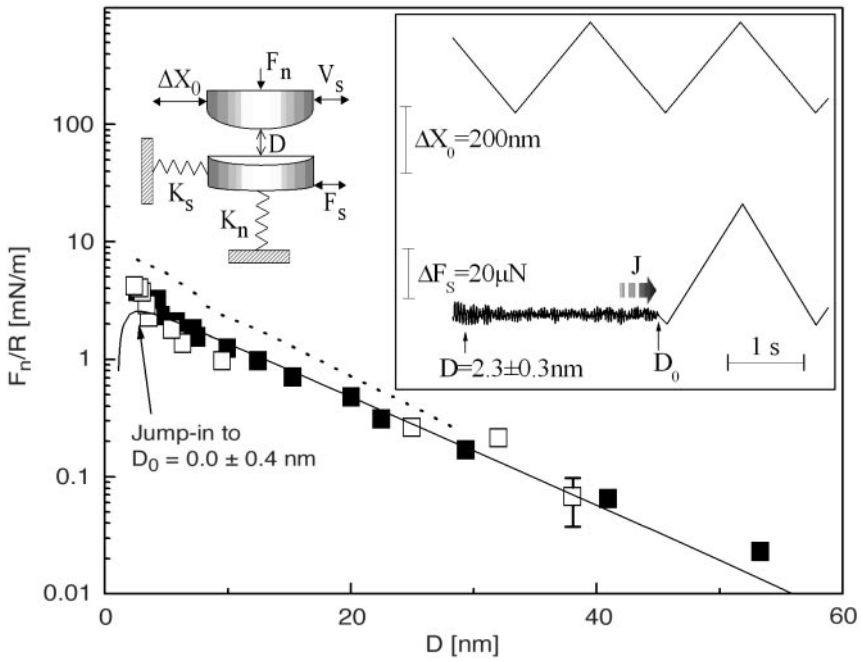

Fig. 1. Interactions across low-concentration aqueous salt solution. The normalized forces F_n/R as a function of closest surface separation D are shown on approach of curved muscovite mica surfaces across $(1 \pm 0.1) \times 10^{-3}$ M NaCl (Mica grade I; S & J Trading Inc., New York, is glued, using Shell EPON 1004F, onto cylindrical quartz lenses with a mean radius of curvature $R = \sim 1$ cm). The top left inset shows schematically the main features of the SFB used (*26*), indicating the two orthogonal springs K_s and K_n whose bending measures directly the shear and normal forces between the surfaces as they are moved laterally parallel ($\pm \Delta x_0$) or normal to each other, respectively. The solid line is the theoretical DLVO fit (*7*) to the $F_n(D)/R$ plot, $F_n/2\pi R = 64 C k_B T \kappa^{-1} \tanh^2(e\psi_0/k_BT) \exp(-\kappa D) - A_H/12\pi D^2$, where $C = 10^{-3}$ is the electrolyte concentration in mol dm^{-3}, T is the temperature (296 ± 1 K), k_B is Boltzmann's constant, A_H is the Hamaker constant of mica across water (2×10^{-20} J), and $\psi_0 = 78$ mV and $\kappa^{-1} = 9.5$ nm are, respectively, the effective (large-separation) surface potential and the Debye length corresponding to the salt concentration used. The broken line is from the study on 1.4×10^{-3} M NaCl (*3*). The right inset shows the applied motion (upper trace) and shear force transmitted between the surfaces (lower trace) as they approach each other under slow thermal drift before jumping (arrow J) from $D = D_j = 2.3 \pm 0.3$ nm into adhesive contact at $D = D_0 = 0 \pm 0.4$ nm, after which they are rigidly adhered and move in tandem (all traces taken directly from the oscilloscope). On separation, the surfaces jump out to $D = 2.8 \pm 0.2$ μm, corresponding to a surface energy $\gamma = -9.8 \pm 0.5$ mN/m (determined from the pull-off force), comparable to earlier reports (*40*, *41*). Before adding the NaCl (Fluka Certified Standard 99.886%) to the required concentration, the zero of the surface separation axis, $D = D_0 = 0$, is determined in conductivity water [for purification details, see (*33*)] and is at a position -0.8 ± 0.3 nm with respect to air contact between the surfaces, based on measurements from four different experiments (*29*).

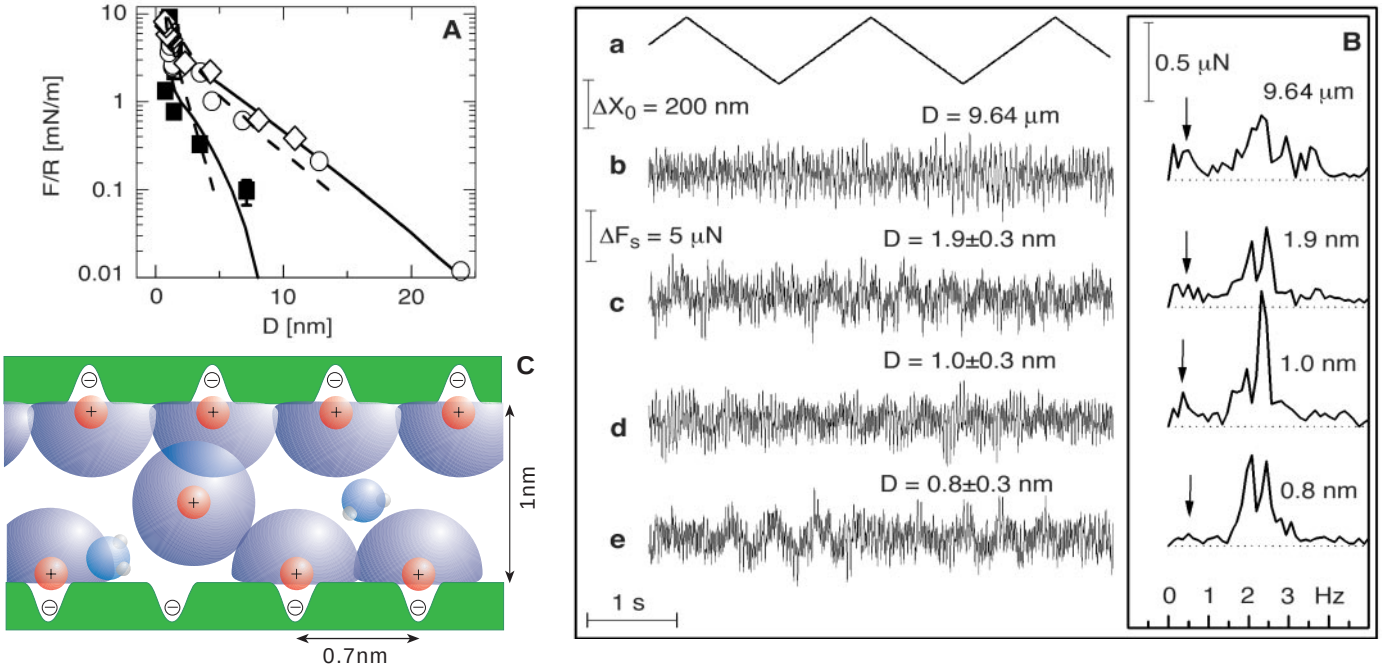

Fig. 2. Interactions across high-concentration aqueous salt solutions. (**A**) Normal forces measured on approach of the surfaces at two different concentrations: $(0.7 \pm 0.2) \times 10^{-2}$ M, empty symbols; and $(0.8 \pm 0.1) \times 10^{-1}$ M NaCl solution, filled symbols, corresponding to the shear traces in (B). The solid lines are a fit to a DLVO expression together with a short-ranged exponential term representing the hydration forces: $F_h/2\pi R = 64Ck_BT\kappa^{-1}\tanh^2(e\psi_0/k_BT)\exp(-\kappa D) - A_H/12\pi D^2 + E_h\exp(-D/D_h)$. The fit values are $\psi_0 = 58$ mV, $\kappa^{-1} = 4.0$ nm, $E_h = 0.1$ J/m^2, and $D_h = 0.35$ nm; and $\psi_0 = 35$ mV, $\kappa^{-1} = 1.8$ nm, $E_h = 0.1$ J/m^2, and $D_h = 0.3$ nm at the lower and higher NaCl concentrations, respectively. The broken lines are from previous studies for the corresponding lower (*3*) and higher (*20*) NaCl concentrations. (**B**) Variation of the shear force response $F_s(D)$ [traces (b) to (e)] with lateral motion of the top surface [trace (a)] for curved mica surfaces sliding past each other across the salt solutions (see schematic in fig. 1), at the D values indicated. The respective salt concentrations for the different traces are as follows: (b), (d) – 0.8×10^{-1} M NaCl; (c), (e) – 0.7×10^{-2} M NaCl. The frequency components of the shear forces corresponding to the traces are shown to the right in (B), with the drive frequency of the top surface (0.5 Hz) indicated by arrows. The peaks around 2.4 Hz correspond to the flexural motion of the building. The cartoon in (**C**) shows, approximately to scale relative to the mica surface separation $D = 1$ nm, the spacing of the ionizable mica surface lattice sites (~0.7 nm) and the size of a free hydrated Na^+ ion [roughly 0.75-nm diameter from bulk studies (*5*), or somewhat smaller for surface-attached ions, as suggested in (*4*)]. Water molecules (diameter ~0.25 nm) are indicated for comparison.

the hydrated sodium ions in the gap is not known, this value (which applies for the two surfaces far apart), together with estimates of the density of the ions on the mica surfaces at these high salt concentrations (*3*), suggests that hydrated Na^+ ions had condensed over nearly all of the ionizable lattice sites (Fig. 2C). Given the size of the hydration sheath surrounding the ions (0.7 to 0.8 nm in the bulk) (*5*), this result shows that at surface separations of 1 nm the gap between the surfaces is occupied mostly by charge-bound water molecules, and that on sliding of the surfaces these bound layers must rub past each other. As shown by our data, the resulting shear forces are characteristic of a fluidity that is not too far removed from that of bulk water. This raises the following question: if the hydrating water layers are so tenaciously bound as to render the film almost solidlike in its reluctance to being squeezed out, thereby preventing approach of the surfaces, how can they at the same time be so fluid, providing striking lubrication as they slide past each other? [In contrast, free or unbound water, which also retains its bulk fluidity down to subnanometer confinement, is readily squeezed out by the confining surfaces as they come into adhesive contact) (Fig. 1) (*33*)].

The answer is unlikely to be related to the mobility of the surface-bound ions themselves (*37*). Rather, it may be attributed to the following. Water molecules are difficult to remove outright from the surface-attached ions to which they are bound, owing to the large energy penalty associated with the increase in the ion self-energy (*5*). However, a much lower energy barrier may be associated with exchange of water molecules at the outer surfaces of the two bound hydration layers. During such an exchange, the remaining bound molecules could rearrange at little entropy cost to minimize the binding charge's self-energy (*5*). This would also be consistent with the rapid exchange of hydration water surrounding monovalent ions in bulk solution (*38*). A corollary is that the hydrated layers act as highly efficient lubricants (*39*). They are capable of supporting a large normal load because on average, the bound water tenaciously adheres to the underlying surface or ions, but the rapid exchange of molecules [which in the bulk liquid occurs at $\sim 10^9$ s^{-1} (*38*)] ensures that the surface-bound hydration layer remains very fluid at the shear rates (up to $\sim 10^3$ s^{-1}) used in our study.

Finally, this fluidity of bound water at salt concentrations and pressures typical of those in living systems has implications for electrolytes under extreme confinement in biological and other naturally occurring systems. Our results indicate that such aqueous species, irrespective of the structural origin of their equilibrium interactions (*6*, *9*, *10*), will have mobilities that do not differ greatly from those in the bulk solution. This is because the conditions of our experiments—confining the ions by hard, smooth, parallel, high-energy surfaces—present an extreme of confinement. This suggests that the fluidity we observe is more than likely to carry over to bound hydration layers in the less stringent, softer environment of biological systems.

References and Notes

1. D. M. LeNeveu, R. P. Rand, V. A. Parsegian, *Nature* **259**, 601 (1976).
2. J. N. Israelachvili, G. E. Adams, *J. Chem. Soc. Faraday Trans. I* **79**, 975 (1978).
3. R. M. Pashley, *J. Colloid Interface Sci.* **83**, 531 (1981).
4. ———, *Adv. Colloid. Interface Sci.* **16**, 57 (1982).
5. P. P. S. Saluja, in *Electrochemistry*, J. O. M. Bockris, Eds. (Butterworths, London, 1976), vol. 6, pp. 2–51.
6. S. Marcelja, *Nature* **385**, 689 (1997).

7. B. V. Derjaguin, N. V. Churaev, V. M. Muller, *Surface Forces* (Plenum, New York, 1987).
8. J. Clifford, in *Water in Disperse Systems*, F. Franks, Eds. (Plenum, New York, 1975), vol. 5, pp. 75–132.
9. V. A. Parsegian, *Adv. Colloid Interface Sci.* **16**, 49 (1982).
10. J. N. Israelachvili, H. Wennerstrom, *Nature* **379**, 219 (1996).
11. M. Gerstein, M. Levitt, *Sci. Am.* **100** (November 1998).
12. I. Ravina, P. F. Low, *Clays Clay Miner.* **20**, 109 (1972).
13. Special Issue on Biolubrication, *Proc. Inst. Mech. Eng. Eng. Med.* **210** (1987).
14. R. N. Barnett, C. L. Cleveland, A. Joy, U. Landman, G. B. Schuster, *Science* **294**, 567 (2001).
15. D. S. Goodsell, *The Machinery of Life* (Springer-Verlag, New York, 1993).
16. M. S. P. Sansom, I. H. Shrivastava, K. M. Ranatunga, G. R. Smith, *Trends Biochem. Sci.* **25**, 368 (2000).
17. Special issue on "The Hydration Problem in Solution Biophysics," S. E. Harding, Ed., *Biophys. Chem.* **93**, 87 (2001).
18. Experiments on hydrodynamic forces between smooth surfaces (*19*, *20*, *23*) reveal bulklike fluidity of aqueous salt solutions (concentrations $\geq$0.01 M) confined down to $D \geq 1.8$ nm, at the onset of strong hydration repulsion. Early tribological measurements (*21*) indicate high viscosity of a confined salt solution already at $D \leq 1.8$ nm, but this may be due to transient effects associated also with much higher-than-expected (*10*) normal forces on a first approach of the mica surfaces in (*21*).
19. A. D. Roberts, D. Tabor, *Proc. R. Soc. London Ser. A* **325**, 323 (1971).
20. J. N. Israelachvili, *J. Colloid Interface Sci.* **110**, 263 (1986).
21. A. M. Homola, J. N. Israelachvili, M. L. Gee, P. M. McGuiggan, *J. Tribol.* **111**, 675 (1989).
22. R. G. Horn, D. T. Smith, W. Haller, *Chem. Phys. Lett.* **162**, 404 (1989).
23. Smaller separations ($D \leq 0.5$ nm) must involve at most only water monolayers or submonolayers directly attached to the solid crystal substrates themselves and likely to be modified relative to layers farther away [see, for example (*24*, *25*)].
24. P. B. Miranda, L. Xu, Y. R. Shen, M. Salmeron, *Phys. Rev. Lett.* **81**, 5876 (1998).
25. L. Cheng, P. Fenter, K. L. Nagy, M. L. Schlegel, N. C. Sturchio, *Phys. Rev. Lett.* **87**, 156103 (2001).
26. J. Klein, E. Kumacheva, *J. Chem. Phys.* **108**, 6996 (1998).
27. D. Tabor, R. H. Winterton, *Proc. R. Soc. London Ser. A.* **312**, 435 (1969).
28. H. Poppa, A. G. Elliot, *Surface Sci.* **24**, 149 (1971).
29. Removal of the air-adsorbed contaminants [which consist of water, gas, and organic contaminants (*28*)] is indicated by adhesive contact in salt-free water at a separation of ~5 to 8 Å farther in relative to air contact [for example (*2*, *21*, *27*, *33*)].
30. M. Wilhelm, X. Zhang, J. Klein, unpublished observations.
31. Y. Zhu, S. Granick, *Phys. Rev. Lett.* **87**, 096104 (2001).
32. Measurements reported in (*31*) indicate an effective viscosity of confined salt solutions (~0.03 M monovalent and divalent salts) already at $D < 2$ to 2.5 nm, which is several orders of magnitude higher than that of bulk water or than that reported here [but is comparable to our earlier measurements of high viscosities at similar D values (*30*)]. We do not know the reasons for this large discrepancy with our present results, but note that the controls indicating removal of air-adsorbed contaminant layers (*29*) are not reported in (*31*).
33. U. Raviv, P. Laurat, J. Klein, *Nature* **413**, 51 (2001).
34. When much higher loads ($F/R > 10^4$ μN/m) were applied, we found that under shear—and only when sheared—the surfaces clearly appeared to damage, exhibiting large and erratic frictional forces and indications of debris on subsequent separation and approach. Such damage was observed in both (0.7 ± 0.2) $\times 10^{-2}$ M and (0.8 ± 0.1) $\times 10^{-1}$ M NaCl solutions and when KNO_3 solutions in the hydration-repulsion regime were examined at higher loads. Similar damage at high loads between compressed mica surfaces across aqueous salt solutions was reported previously (*35*).
35. P. M. McGuiggan, R. M. Pashley, *J. Phys. Chem.* **92**, 1235 (1988).
36. The compressive forces result in a flattened region between the surfaces of area A. Direct measurement of the flattened area from the fringe shape gives $A = (2.8 \pm 0.7) \times 10^{-10}$ m^2; applying the JKR (Johnson, Kendal, and Roberts) contact mechanics relation, $A \approx \pi(RF_n/K)^{2/3}$, where $R \approx 1$ cm is the mean radius of curvature of the mica surfaces and $K = (1 \pm 0.3) \times 10^9$ N/m^2 is an effective modulus of the surfaces (*26*) gives the very similar value $A = (3 \pm 0.3) \times 10^{-10}$ m^2 for $D = 1$ nm. The effective viscosity is obtained from the Newtonian relation $\sigma_s = \eta_{eff}(v_s/D)$, where the shear stress is given by $\sigma_s = (F_s/A)$ and (v_s/D) is the shear rate (the shear velocity v_s going up to 1200 nm·s^{-1} in this study). The upper limit σ_s^{upper} on the mean shear stress required to slide the surfaces at this velocity is set by $F_s \leq \delta F_s$, giving $\sigma_s^{upper} \leq \sim 100$ N/m^2.
37. G. L. Gaines, D. Tabor, *Nature* **178**, 1304 (1956).
38. F. A. Cotton, G. Wilkinson, *Advanced Inorganic Chemistry* (Wiley, New York, ed. 5, 1998), pp. 1288–1289.
39. An effective friction coefficient μ_{eff} may be defined as $\mu_{eff} = (F_s/F_n)$, where F_s is the force required to slide the surfaces under a load F_n. This value is resolution limited by $F_s \leq \delta F_s$, giving at $D = D_c$ the remarkably low upper limit $\mu_{eff} \leq \sim 0.0002$ at the shear rates (~300 s^{-1}) and pressures ($F_n/A = \sim 4$ atm) corresponding, for example, to traces (d) or (e) in Fig. 2B.
40. P. M. McGuiggan, J. N. Israelachvili, *J. Mater. Res.* **5**, 2232 (1990).
41. U. Raviv, P. Laurat, J. Klein, *J. Chem. Phys.* **116**, 5167 (2002).

42. We thank N. Kampf for experimental help; we appreciate comments on the manuscript by J. Israelachvili and S. Safran, and thank D. Lukatski, T. Witten, P. Pincus, A. Zilman, and P.-G. de Gennes for useful discussions. Support by the Eshkol Foundation (U.R.), the Deutsche-Israel Program, and the United States-Israel Binational Science Foundation is gratefully acknowledged.

29 May 2002; accepted 26 July 2002

Natural Product Terpenoids in Eocene and Miocene Conifer Fossils

Angelika Otto,[1]*† James D. White,[2] Bernd R. T. Simoneit[1]

Numerous saturated and aromatic hydrocarbons, but not polar compounds, originating from plants and microorganisms (biomarkers) have been reported in sediments, coals, and petroleum. Here we describe natural product terpenoids found in two fossil conifers, *Taxodium balticum* (Eocene) and *Glyptostrobus oregonensis* (Miocene). A similar terpenoid pattern is also observed in extant *Taxodium distichum*. The preservation of characteristic terpenoids (unaltered natural products) in the fossil conifers supports their systematic assignment to the Cypress family (Cupressaceae sensu lato). The results also show that fossil conifers can contain polar terpenoids, which are valuable markers for (paleo)chemosystematics and phylogeny.

Most sediments contain solvent-extractable organic compounds that are derived from natural product precursors biosynthesized by living organisms. These biomolecules are degraded before and after burial in sediments to their diagenetic products (geomolecules). Despite various chemical transformations, the geomolecules retain their characteristic basic structural skeletons and can thus be used as biomarkers for their biological origin. Such biomarkers can provide information on the source of organic matter in sediments, paleoclimate, and gas and coal geochemistry, and they can be used as tracers in environmental studies (*1*–*4*). Most of the previous studies have focused on the saturated and aromatic biomarker hydrocarbons. Because the degradation of numerous polar precursor molecules may result in the generation of the same hydrocarbon product (*5*, *6*), the hydrocarbons are characteristic only for wider groups of organisms, such as conifers, angiosperms, or bacteria. In contrast, only slightly degraded or unaltered polar compounds are more specific biomarkers, because the natural product precursors have a distinct distribution in living organisms. For this reason, the composition of polar compounds in geological samples is of particular significance. The preservation potential of polar compounds in sediments is believed to be very low (*7*) because they generally undergo rapid diagenetic processes, such as degradation, reactions with other compounds, or bonding to the insoluble kerogen (*8*). Here we show that polar terpenoids can be preserved as unaltered natural products in fossil conifers and discuss their implications for chemosystematics and phylogeny.

[1]Environmental and Petroleum Geochemistry Group, College of Oceanic and Atmospheric Sciences, Oregon State University, Corvallis, OR 97331, USA. [2]Department of Chemistry, Oregon State University, Corvallis, OR 97331, USA.

*Present address: Johann Wolfgang Goethe-Universität Frankfurt/Main, Institut für Mineralogie–Umweltanalytik, Georg-Voigt-Strasse 14, D-60054 Frankfurt/Main, Germany.

†To whom correspondence should be addressed. E-mail: a.otto@kristall.uni-frankfurt.de